



HAL
open science

Measurement of atmospheric production depths of muons with the pierre auger observatory

D. Garcia-Gamez

► **To cite this version:**

D. Garcia-Gamez. Measurement of atmospheric production depths of muons with the pierre auger observatory. International Symposium on Future Directions in UHECR Physics (UHECR 2012), Feb 2012, Geneva, Switzerland. pp.04008, 10.1051/epjconf/20135304008 . in2p3-00682717

HAL Id: in2p3-00682717

<https://in2p3.hal.science/in2p3-00682717v1>

Submitted on 27 Jun 2013

HAL is a multi-disciplinary open access archive for the deposit and dissemination of scientific research documents, whether they are published or not. The documents may come from teaching and research institutions in France or abroad, or from public or private research centers.

L'archive ouverte pluridisciplinaire **HAL**, est destinée au dépôt et à la diffusion de documents scientifiques de niveau recherche, publiés ou non, émanant des établissements d'enseignement et de recherche français ou étrangers, des laboratoires publics ou privés.

Measurement of atmospheric production depths of muons with the pierre auger observatory

D. García-Gómez¹ for the Pierre Auger Collaboration^{2,a}

¹ *Laboratoire de l'Accélérateur linéaire (LAL), Université Paris 11, CNRS-IN2P3, Orsay, France*

² *Observatorio Pierre Auger, Av. San Martin Norte 304, 5613 Malargüe, Argentina*
(Full author list: http://www.auger.org/archive/authors_2012_06.html)

Abstract. The time structure of muons at ground retains valuable information about the longitudinal development of the hadronic component in extensive air showers. Using the signals collected by the surface detector array of the Pierre Auger Observatory it is possible to reconstruct the Muon Production Depth (MPD) distribution. In this work we explore the main features of these reconstructions for zenith angles around 60° and different energies of the primary particle. From the MPDs we define a new observable, X_{\max}^μ , as the depth, along the shower axis, where the maximum number of muons is produced. The potentiality of X_{\max}^μ to infer the mass composition of cosmic rays is studied.

1. INTRODUCTION

The Pierre Auger Observatory [1] is a hybrid detector that combines both surface (SD) [2] and fluorescence (FD) [3, 4] detectors at the same site. It allows to measure the longitudinal profile of ultra-high energy air showers and the depth at which the shower reaches its maximum size, X_{\max} [5], and also provides a record of the shower front by sampling the secondary particles at ground level. The FD operates only on clear, moonless nights, so its duty cycle is small (about 13%). The SD has a duty cycle close to 100%. This translates into a large increase in statistics that makes very useful the use of SD observables to study the composition of Ultra-High Energy Cosmic Rays (UHECR).

Most of the muons produced in extensive air shower (EAS) come from the decay of pions and kaons. Muons are born along a narrow neighborhood around the shower axis [6]. Interactions as bremsstrahlung or pair production are improbable and multiple scattering effects are nearly negligible because of their high energies. It is therefore reasonable to assume that muons travel following straight lines. So the time structure of muons at ground still retains information about their production points. Based on all this, [6, 7] present a model where the muon production depth (MPD) along the shower axis is reconstructed. In this work we show that MPDs provide a physical observable that can be used as a sensitive parameter to study the chemical composition of cosmic rays [8].

2. MPD RECONSTRUCTION

References [6, 7] propose a model where it is possible to infer the muon production distance, z , along the shower axis, starting from the FADC traces measured by the surface detectors. From Figure 1 and assuming muons travel undeflected at the speed of light, c , from birth until reaching the ground, it is

^aFor the full authorlist see Appendix “Collaborations” in this volume.

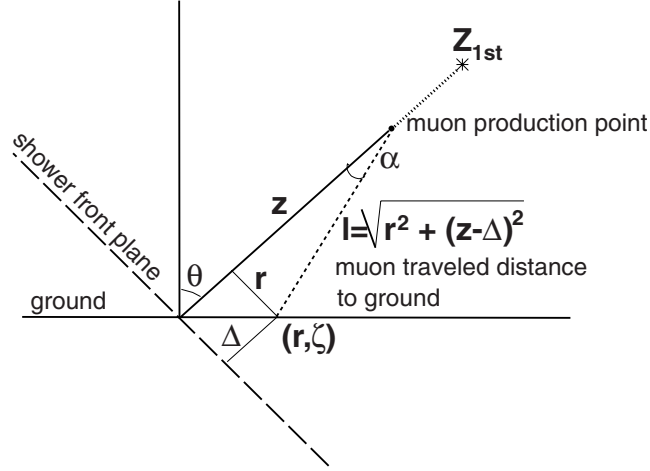


Figure 1. Picture of the geometry used to obtain the muon traveled distance and the geometrical delay.

possible to derive:

$$z = \frac{1}{2} \left(\frac{r^2}{ct_g} - ct_g \right) + \Delta \quad (1)$$

where r is the distance from the point at ground to the shower axis, Δ is the distance from the same point to the shower plane and t_g (*geometrical delay*) is the time delay with respect to the arrival of the shower front plane. The shower front plane is defined as the plane perpendicular to the shower axis and moving at c in the direction of the shower axis. To avoid an underestimation of the muon production distance z (from Equation 1) we must take into account the energy of the muons. This translates into an extra contribution to the total delay $ct = ct_g + ct_e(E)$. To know the *kinematic delay*, t_e , we need to estimate each single muon energy. Given that these energies are not measurable with the actual array detectors, t_e is approximated by an averaged value, that must be subtracted from the measured time delay prior to the conversion into z , as described in [6, 7]. The kinematical contribution to the delay dominates at short distances to the core, where the geometrical time delay is very small. At large distances ($r > 600$ m) t_e acts as a correction (typically below 20%).

Equation 1 gives a mapping between the production distance z and the *geometrical delay* t_g for each point at ground. The production distance can be easily related to the total amount of traversed matter X^μ using

$$X^\mu = \int_z^\infty \rho(z') dz' \quad (2)$$

where ρ is the atmosphere density. This X^μ distribution is referred to as MPD-distribution. The shape of the MPD-distribution contains relevant information about the development of the hadronic cascade and the first interaction point. To extract valuable physics insight from the MPD we perform a fit. To describe the shape of the MPD-profile we use a Gaisser-Hillas function [9]. The fit with this function provides the maximum of the distribution, X_{\max}^μ . We interpret X_{\max}^μ as the point where the production of muons reaches the maximum along the cascade development. In this work we demonstrate that this new observable can be used for composition studies.

The MPD-distribution is populated with the surviving muons reaching ground, so the muon decay probability shapes the distributions differently depending on the zenith angle. Furthermore, different points at ground sample different stages of the shower development. Hence, the reconstructed profiles also change with the distance to the core. These features are shown in Figure 2. It displays simulated

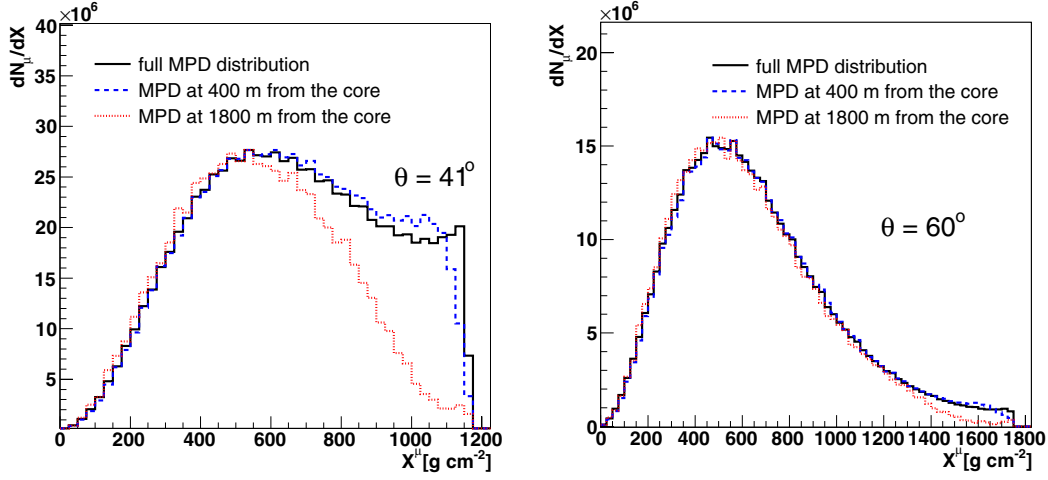


Figure 2. Muon production depth (MPD) distributions extracted from an iron shower of 10^{19} eV simulated with AIRES [10] at two different zenith angles: 41° (left) and 60° (right). The MPD dependence with the distance to the core is shown. Similar conclusions apply in the case of showers originated by protons.

MPD-distributions for an iron primary at two different zenith angles and at different distances from the core, r . The shape of the MPD-distributions clearly depends on the shower inclination. For angles of about 40° and lower, the reconstructed profile, and therefore its maximum, are very different depending on the value of r . At large zenith angles, showers develop higher in the atmosphere and the dependence of the MPDs with the core location is reduced, becoming negligible (X_{\max}^μ varies less than 10 g cm^{-2}) around 60° and above. Thus, for those showers the reconstruction can be done just by adding the X^μ distributions from the different surface detectors. At small zenith angles, this addition requires the introduction of a correction factor to transform the distributions observed at the different core distances to the one expected at a reference r (see [6, 7] for a thorough discussion about this correction). The positive correlation between the zenith angle and the values of z makes the accuracy of the reconstruction becomes worse for more horizontal events (see Equation 3 in next section). For all the previous reasons we select for our analysis data with measured zenith angles between 55° and 65° .

2.1 Detector effects

The precision of the method is limited so far by the detector capabilities. The sampling rate in the FADC traces produces an uncertainty on the z reconstruction that decreases quadratically with r (the distance to the core), and increases linearly with z as:

$$\frac{\delta z}{z} \simeq 2 \frac{z}{r^2} c \delta t. \quad (3)$$

Note that this uncertainty is linked to each single time bin entry of the FADC traces. The total uncertainty of the MPD maximum, δX_{\max}^μ , depends not only on δX (δz) but also on the number of muons N_μ , and therefore decreases as the square root of N_μ . To keep the distortions on the reconstructed MPD small, only tanks far from the core can be used. The cut in r diminishes the efficiency of the reconstruction as the number of muons is reduced. As r_{cut} increases we might not have enough muons (or no muons at all) to properly reconstruct the MPD-profile. On the other hand, the efficiency in the reconstruction will increase as we increase the energy of the shower (because more muons are produced), and will be higher for heavy than for light primaries. Hence a r_{cut} value must be carefully chosen in order to guarantee good reconstruction efficiencies, avoiding at the same time a bias on the mass of the primary.

Furthermore, signals collected by the water Cherenkov detectors are the sum of the electromagnetic (EM) and muonic components. The arrival time distributions are different for both components. Muons produce spikes over the smoother EM contribution in the signals. As a consequence, a cut on signal threshold, rejecting all time bins with signal below a certain value, might help diminishing the contribution of the EM contamination. Moreover, applying a cut in r helps to reduce this undesirable effect since tanks close to the core with signals dominated by the EM component are removed. Note that there is an additional EM component that always accompanies muons and does not show such a strong dependence with the distance to the core. This is sometimes referred as the EM halo, and comes from the decay of muons in flight. This component is harder to avoid, but it follows closer the time distribution of their parent muons, thus it does not hamper our analysis.

2.2 Reconstruction cuts

We have used Monte Carlo simulations to find the optimal conditions for a good reconstruction of the MPDs and an accurate determination of the value of X_{\max}^{μ} . As mentioned above, time resolution forces the use of a cut in core distance. The more we move away from the core, the better the resolution in determining the depth, X , but the lower the number of muons contributing to the reconstruction. The best balance between these conflicting requirements was found for a r_{cut} bigger than 1800 m. This cut alone is not enough to get rid of the residual EM contamination and potential baseline fluctuations that distort the shape of the MPD-distribution. For this reason a cut in the threshold of the FADC traces is applied. Time bins with a signal below 0.3 VEM are removed. Finally, to minimize the impact on the analysis due to detectors dominated by possible accidental particles (normally very far away from the core), we impose that the total recorded signal by each detector contributing to the MPD-profile should be larger than 3 VEM.

After applying all these cuts, the muon selection efficiency is very high. Regardless of the energy of the primary and its composition, muon fractions above 85% are always obtained. This guarantees an EM contamination low enough to obtain an accurate value of X_{\max}^{μ} .

2.3 Selection cuts

Once the MPD-distribution is reconstructed for each individual event, we must optimize our selection with a set of simple quality cuts. They are the following:

- **Trigger cut:** All events must fulfill the T5 trigger condition [2].
- **Energy cut:** The number of muons detected at ground increases with the energy of the event but decreases with the distance to the core as $N_{\mu} \propto E^{\alpha}/r^{\beta}$. Based on simulations, we have observed that the number of muons contributing to the reconstruction of a MPD-distribution is very small for events with energies below 20 EeV. This results in a very poor determination of the X_{\max}^{μ} observable. Therefore, our analysis is restricted to events with energy larger than 20 EeV.
- **Fit quality:** Only events with a good MPD-profile fit ($\chi^2/\text{ndf} < 2.5$) to a Gaisser-Hillas function are accepted.
- **Shape cut:** The reduced χ^2 of a straight line and a Gaisser-Hillas fit must satisfy $\chi_{GH}^2/\text{ndf} < 2\chi_{line}^2/\text{ndf}$.

Table 1 displays a summary of the Monte Carlo efficiencies, using the hadronic interaction model QGSJETII, for proton and iron primaries at different energies. The overall event selection efficiencies are high (>80%) and our cuts do not introduce any appreciable composition bias. We finally note that for the set of surviving events, the bias in the X_{\max}^{μ} reconstruction is between $\pm 10 \text{ gcm}^{-2}$, across our range of energies regardless of the primary. Figure 3 shows the evolution with energy of the actual RMS of the distribution obtained when computing the difference, on an event by event basis, between the measured (reconstructed) and true (generated) X_{\max}^{μ} , for the case of pure proton or iron composition at

Table 1. Selection efficiencies for proton and iron QGSJETII Monte Carlo showers as a function of energy.

$\log_{10}(E/eV)$	ε_p (%)	ε_{Fe} (%)	$ \varepsilon_p - \varepsilon_{Fe} $ (%)
19.25	82	87	6
19.50	84	86	2
19.75	85	82	3
20.00	95	97	2

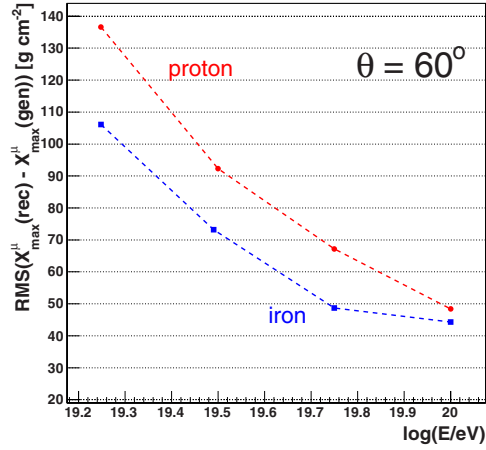


Figure 3. Energy evolution of the resolution we obtain, on an event by event basis, when we reconstruct X_{\max}^{μ} for showers generated with AIRES and QGSJETII [11].

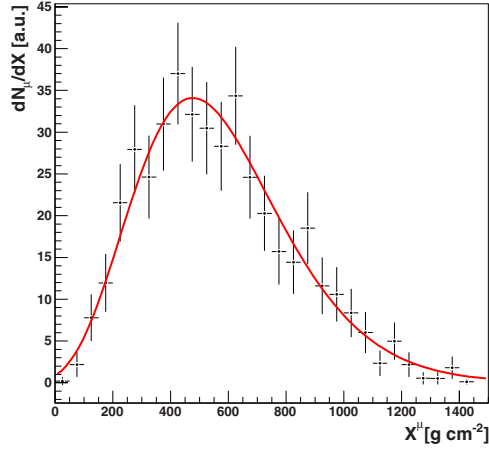


Figure 4. Example of a real reconstructed MPD, $\theta = (59.05 \pm 0.07)^{\circ}$ and $E = (94 \pm 3)$ EeV, with its fit to a Gaisser-Hillas function.

a zenith angle of 60° . The resolution ranges from about 120 gcm^{-2} at the lower energies to less than 50 gcm^{-2} at the highest energy. Thanks to the increase with energy on the number of muons reaching ground, this RMS decreases and converges to a similar value for iron and proton.

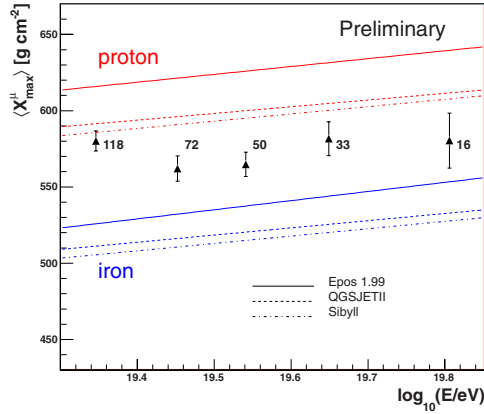


Figure 5. $\langle X_{\max}^{\mu} \rangle$ as a function of the energy. The number of real data events in each energy bin is indicated. The predictions for proton and iron following different hadronic models are shown as well.

Table 2. Evaluation of the main sources of systematic uncertainties.

Source	Sys. Uncertainty (g cm^{-2})
Reconstruction bias	9.8
Atmospheric Uncertainty	8.5
Core position	4.8
EM contamination	1.5
χ^2 cut	0.2
Selection efficiency	1
Total	14

3. APPLICATION TO REAL DATA

The analysis shown in this document is an update from the work presented in [12] including one more year of real data. Furthermore, we have improved the accuracy of the atmospheric density profiles used for the translation from distance (z) to depth (X). Now we use atmospheric data from the Global Data Assimilation System (GDAS) [13], with a time resolution of 3 hours, instead of a fixed averaged profile. In the present work we analyze data collected between January 2004 and October 2011. We start from a sample of 457 events with reconstructed energy bigger than 20 EeV and zenith angle $\theta \in [55^\circ, 65^\circ]$. The overall selection efficiency amounts to about 63%, resulting in 289 surviving events. The difference between the efficiencies shown in Table 1 and the selection efficiency in real data is due to the T5 cut [2]. This cut has an efficiency of about 77% for data, while all our Monte Carlo showers are generated as T5 events. The reconstruction for one of our more energetic events is shown in Figure 4. Figure 5 shows the evolution of the $\langle X_{\max}^{\mu} \rangle$ observable as a function of energy. Each bin has a width of 0.1 in $\log_{10}(E/\text{eV})$, except the last one which contains all the events with energy larger than $\log_{10}(E/\text{eV})=19.7$. The error bars correspond to the standard deviation on the mean. If compared to air shower predictions using standard interaction models, our measurement is compatible with a mixed composition. The same conclusion was found in the analysis reported at [12]. This interpretation could change if the discrepancy between models and data [14] is not limited to the *total* number of muons but to their energies and spatial distributions.

The most relevant contributions to the systematic uncertainties are summarized in Table 2. The uncertainties on the MPD reconstruction and event selection translate into a systematic uncertainty on $\langle X_{\max}^{\mu} \rangle$ of 14 g cm^{-2} .

4. CONCLUSIONS

It is possible to reconstruct the muon production depth distribution using the FADC traces of the SD detectors far from the core. From the MPDs we define a new observable X_{\max}^{μ} . It represents the observed depth along the shower axis where the number of produced muons reaches a maximum. The applicability of this observable and its resolution for zenith angles $\sim 60^{\circ}$ have been characterized for different shower energies. We have demonstrated, for the first time, that X_{\max}^{μ} is a parameter sensitive to the mass composition of UHECR. The result of this study is in agreement with all previous Auger results [15] obtained with other completely independent methods and having a different set of systematic uncertainties.

References

- [1] The Pierre Auger Collaboration, Nucl. Instr. and Meth. A **523** (2004) 50–95
- [2] The Pierre Auger Collaboration, Nucl. Instr. and Meth. A **613** (2010) 29–39
- [3] The Pierre Auger Collaboration, Nucl. Instr. and Meth. A **620** (2010) 227–251
- [4] H.-J. Mathes for the Pierre Auger Collaboration, Proc. 32nd ICRC, Beijing, China **5** (2011)
- [5] The Pierre Auger Collaboration, Phys. Rev. Lett. **104** (2010) 1–7
- [6] L. Cazon, R.A. Vazquez, A.A. Watson, E. Zas, Astropart. Phys. **21** (2004) 71–86
- [7] L. Cazon, R.A. Vazquez, E. Zas, Astropart. Phys. **23** (2005) 393–409
- [8] D. Garcia-Gamez, Universidad de Granada, PhD Thesis, (2010)
- [9] T. K. Gaisser and A. M. Hillas, Proc. 15nd ICRC, Plovdiv, Bulgaria **8** (1997) 13–26
- [10] S. Sciutto, Proc. 27th ICRC, Hamburg, Germany, (2001)
- [11] S. Ostapchenko, Proc. AIP Conference, Granlibakken, USA **928** (2007) 118–125
- [12] D. Garcia-Gamez for the Pierre Auger Collaboration, Proc. 32nd ICRC, Beijing, China **2** (2011)
- [13] The Pierre Auger Collaboration, Astropart. Phys. **35** (2012) 591–607
- [14] J. Allen for the Pierre Auger Collaboration, Proc. 32nd ICRC, Beijing, China **2** (2011)
- [15] D. Garcia-Pinto for the Pierre Auger Collaboration, Proc. 32nd ICRC, Beijing, China **2** (2011)